Probing dissociative electron attachment through heavy-Rydberg ion-pair production in Rydberg atom collisions

S. Buathong, M. Kelley, and F. B. Dunning
Department of Physics and Astronomy, Rice University, Houston, Texas 77005-1892, USA

(Received 18 August 2016; accepted 23 September 2016; published online 7 October 2016)

Electron transfer in collisions between low-n, $n = 12$, Rydberg atoms and targets that attach low-energy electrons can lead to the formation of heavy-Rydberg ion-pair states comprising a weakly-bound positive-negative ion pair that orbit each other at large separations. Measurements of the velocity and angular distribution of ion-pair states produced in collisions with 1,1,1-$C_2Cl_3F_3$, $CBrCl_3$, BrCN, and $Fe(CO)_5$ are used to show that electron transfer reactions furnish a new technique with which to examine the lifetime and decay energetics of the excited intermediates formed during dissociative electron capture. The results are analyzed with the aid of Monte Carlo simulations based on the free electron model of Rydberg atom collisions. The data further highlight the capabilities of Rydberg atoms as a microscale laboratory in which to probe the dynamics of electron attachment reactions. *Published by AIP Publishing.* [http://dx.doi.org/10.1063/1.4964326]

I. INTRODUCTION

Many molecules capture low-energy electrons leading to reactions of the form

$$\rightarrow A^- + BC \quad (1)$$

$$ABC + e^- \rightarrow ABC^{-*} \rightarrow AB^- + C \quad (2)$$

$$\rightarrow ABC^-, \quad (3)$$

where ABC^{-*} denotes the short-lived excited intermediate formed by initial electron capture and ABC^- a long-lived metastable parent anion formed by intramolecular vibrational relaxation. The dynamics of dissociative attachment, specifically the lifetimes and decay energetics of the ABC^{-*} intermediate, have been the subject of much interest. Here we explore the information on such reactions that can be obtained from studies of heavy-Rydberg ion-pair formation through electron transfer in collisions between the Rydberg atoms and the attaching targets 1,1,1-$C_2Cl_3F_3$, CCl_3Br, BrCN, and $Fe(CO)_5$.

Collisions between Rydberg atoms and neutral targets are frequently discussed using the essentially free electron model because, for sufficiently large values of n, the ranges of the Rydberg electron-target and core ion-target interactions become less than the size of the atom, whereupon the atom behaves as a pair of independent scatterers. Thus studies of collisions dominated by the Rydberg electron-target interaction can provide information on electron-molecule scattering at energies characteristic of the Rydberg electron. Studies of electron transfer in high-n ($n \gtrsim 40$) Rydberg collisions have been used to measure rate constants for electron attachment to a wide variety of molecules at thermal and sub-thermal electron energies, the atom serving essentially as a low-energy electron trap.[1,2] As n decreases, however, the Rydberg electron cloud shrinks and the positive-negative ion pairs created through electron transfer are formed at ever smaller separations resulting in increased post-attachment electrostatic interactions between them. As a result, for thermal energy collisions, an increasing fraction of the ion pairs possess insufficient kinetic energy of relative motion to overcome their mutual electrostatic attraction and separate. They therefore remain bound creating an ion-pair molecular state in which the ions orbit each other at relatively large internuclear separations. Since many of their properties parallel those of Rydberg atoms, such states are often termed as heavy-Rydberg states.[3–7] Rydberg atom collisions have been used to produce a wide variety of ion pair states for the study of their physical and chemical properties.[8–14] We demonstrate here that the production of ion-pair states through dissociative electron transfer reactions of the type,

$$K(12p) + ABC \rightarrow K^+ + ABC^{-*} \rightarrow K^+..A^- + BC \quad (4)$$

$$\rightarrow K^+..BC^- + A, \quad (5)$$

where $K^+..A^-$ and $K^+..BC^-$ denote ion pair states, can also be used to elucidate the dynamics of dissociative electron capture itself. The experimental data are analyzed with the aid of a Monte Carlo collision code that models the detailed kinematics of electron transfer reactions. The model calculations show that the predicted velocity and angular distributions of the product ion-pair states depend on the assumed lifetime and decay energetics of the excited ABC^{-*} intermediate allowing information on these parameters to be obtained through comparison to experimental data. The results further demonstrate the capabilities of Rydberg atoms as a microscale laboratory to probe electron attachment reactions.

II. METHODOLOGY

The present apparatus is shown in Fig. 1. Potassium atoms contained in a collimated beam are photoexcited to the 12p $^2P_{3/2}$ Rydberg state near the center of a small gas cell where they interact with the target gas. A fraction of the

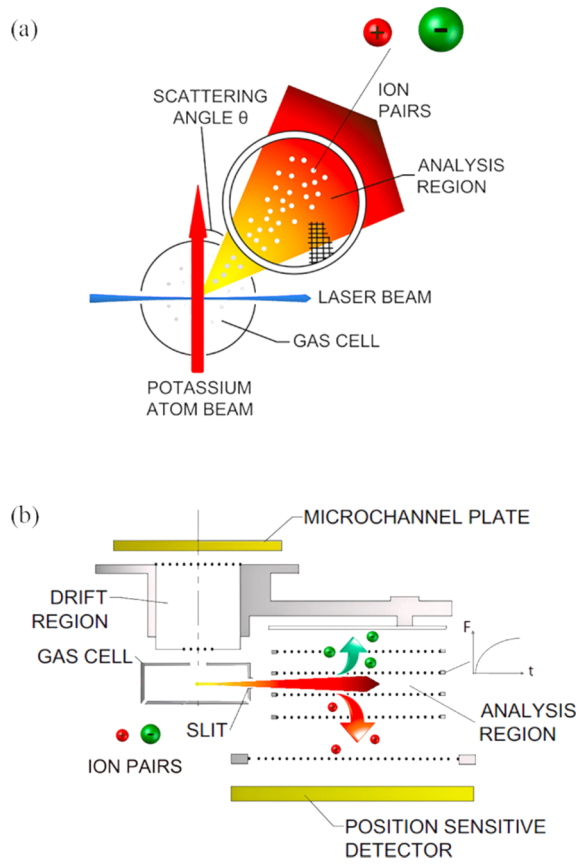

FIG. 1. Schematic diagram of the apparatus. (a) Top view in the *xy* plane defined by the atom and laser beams. Ion pairs traveling in the *xy* plane with scattering angles θ of 22.5°–67.5° exit the gas cell through a slit and enter the analysis region. (b) Side view in a plane through the center of the gas cell and analysis region.

bound ion pairs formed traveling in the *xy* plane defined by the laser and atom beams exit the gas cell through a narrow slit and enter the analysis region where they are detected through dissociation induced by the application of a pulsed electric field. The resulting positive ions are accelerated to a position-sensitive detector (PSD) that records both their arrival times and positions. Time-of-flight techniques are employed to determine the ion-pair velocity distributions. Short pulses of Rydberg atoms are created which undergo rapid collisional destruction forming ion pairs. Position distributions for those ions pairs that enter the analysis region are recorded as a function of the time delay, t_D, between Rydberg atom production and application of the pulsed dissociation field. These distributions are then compared to the results of model calculations undertaken using different assumed intermediate lifetimes and decay energetics to determine the behavior of the intermediates.

The Rydberg atoms are created using 294 nm UV radiation provided by an extracavity-doubled CW Rh6G laser whose output is focused at the center of the gas cell to a diameter of 500 μm and is chopped using an acousto-optic modulator into a series of ~10 μs-duration pulses with a pulse repetition frequency of ~1 kHz. (n = 12 Rydberg atoms were selected for study because they offer relatively high photoexcitation rates and because the majority of the product ion pairs are bound, a reasonable fraction of these having binding energies that allow their dissociation in modest (~5 kV cm^{-1}) electric fields.) To help tune the laser to the desired state, positive ions produced in the gas cell through collisions or blackbody-radiation-induced photoionization are extracted by a small transverse electric field and detected by a microchannel plate. (This field also prevents free ions formed in the gas cell from escaping through the slit and entering the analysis region.)

A fraction of those ion pairs formed traveling within ±4° of the *xy* plane exit the gas cell through a slit that defines "scattering angles," θ, defined as the angle between the initial direction of travel of the Rydberg atom and the trajectory of the ion pair, of ~22.5°–67.5°. They then enter the analysis region which is bounded by two fine-mesh grids where they are dissociated by a pulsed electric field. The resulting K^+ ions are detected by the PSD. For ion pair states with a given binding energy, E_B, field-induced dissociation can occur over a sizable range of fields governed by the values of their angular momentum, L, and its projection, L_z, along the z axis defined by the applied field. However, while it is not possible to assign a unique value of E_B to states that dissociate in a particular field, as discussed elsewhere,[15] a "typical" value for the binding energy of states that dissociate in a field F is given by

$$E_B(\text{meV}) = 14[F(\text{kV cm}^{-1})]^{1/2}. \quad (6)$$

The present applied fields are thus sufficient to dissociate states with typical binding energies of up to ~30 meV. Since only a small fraction of the product ion pairs enter the analysis region, data must be accumulated following many laser pulses to build up the distribution of ion arrival positions, i.e., the initial spatial distributions of the ion pairs themselves.

The measured arrival position distributions are analyzed using a Monte Carlo collision code that models the reaction dynamics.[16] Electron transfer is viewed as resulting from a binary interaction between the Rydberg electron and the target molecule. The initial velocities of the Rydberg atom and a target molecule are chosen at random from their velocity distributions. The probability of electron capture at some point during collision is taken to be proportional to the local electron probability density. (To account for the quantum defect for K(np) states, $\delta \sim 1.71$, the experimental data for a particular K(np) state are compared to model predictions calculated using $(n-2)$p hydrogenic wave functions.) Following attachment, the classical motion of the K^+ ion and the intermediate negative ion is computed. After some time, governed by the lifetime, τ, of the intermediate, the intermediate is presumed to dissociate. If τ is short, i.e., if the electron is captured directly into an antibonding orbital, the great majority of the excess energy of reaction will appear in translation resulting in a narrow translational energy release distribution centered near the excess energy. In contrast, if the intermediate is longer lived, redistribution of the excess energy within the intermediate can occur prior to dissociation and part of the excess energy can appear as rovibrational excitation of the fragments rather than in translation. In the limit of complete statistical redistribution of the excess energy within the intermediate, unimolecular decay theory predicts a Boltzmann-like translational energy release distribution of

the form $e^{-\epsilon/\bar{\epsilon}}$, where $\bar{\epsilon}$ is the mean translational energy release.[17,18] Upon dissociation, the angular distribution of the fragments is taken to be isotropic in the rest frame of the intermediate. The kinetic energy of relative motion of the product ion pair is computed to determine the final (kinetic plus potential) energy of the ion pair and whether or not it is bound. If bound, the final ion pair velocity is calculated. Ion pairs that travel into the analysis region are identified and, by analyzing many collision events, their spatial (and binding energy) distribution is calculated as a function of time delay t_D taking into account the fact that, if the ion pairs have finite lifetimes, some will decay prior to detection in the analysis region. Following the dissociation of an ion pair in the analysis region, the trajectory of the resulting positive ion as it travels to the PSD is computed using SIMION[19] and its arrival position determined. Ion arrival position distributions are built up by considering many collision events. Simulations using different assumed intermediate decay energetics and lifetimes are generated to evaluate how sensitive the arrival position distributions are to these parameters and for comparison to experimental data.

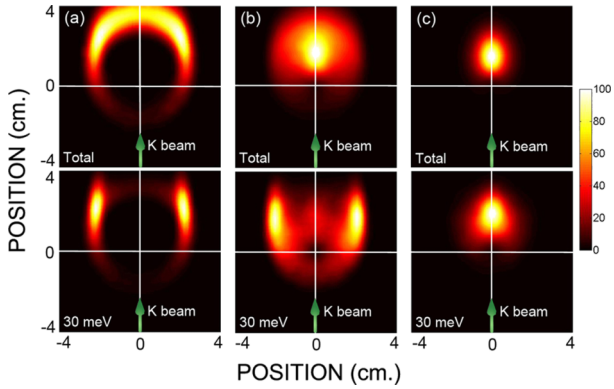

FIG. 2. Calculated position distributions for $K^+..Cl^-$ ion pairs produced in K(12p)–$C_2Cl_3F_3$ collisions that travel within ±4° of the *xy* plane and an ion pair flight time of 40 μs. The ion pair states are initially produced at the origin of the coordinate system. The initial velocity of the Rydberg atoms is indicated. Results in the upper panel refer to the total ion pair production, and those in the lower panel production of ion pair states with binding energies $\lesssim$30 meV. Data are included assuming (a) a δ-function translational energy release centered on 0.35 eV, (b) a flat rectangular distribution extending from 0 to 0.35 eV, and (c) a Boltzmann-like distribution with $\bar{\epsilon} = 0.05$ eV (see text).

III. RESULTS AND DISCUSSION

In collisions with Rydberg atoms, the total excess energy of reaction, E_E, is given by

$$E_E = EA_- - D_0(\text{A-BC}) + E_{int} + E_K(e^-), \tag{7}$$

where EA_- is the electron affinity of the product negative ion, D_0(A-BC) is the A-BC bond dissociation energy, E_{int} is the usable internal energy in the target molecule, and $E_K(e^-)$ is the median kinetic energy of the attached Rydberg electron, ~0.03 eV for the present n value.[2] In the following, the emphasis is on investigating how the excess energy of reaction is distributed between translational and internal motions which, in turn, is related to the lifetime of the ABC^{-*} intermediate.

A. 1,1,1-$C_2Cl_3F_3$

Collisions with 1,1,1-$C_2Cl_3F_3$ result in the formation of ion-pair states through the reaction

$$\begin{aligned} K(12p) + C_2Cl_3F_3 &\rightarrow K^+ + C_2Cl_3F_3^{-*} \\ &\rightarrow K^+..Cl^- + C_2Cl_2F_3. \end{aligned} \tag{8}$$

Two values of the $C_2Cl_2F_3$–Cl bond dissociation energy have been reported, 3.08 eV and 3.19 eV.[20] These, coupled with the electron affinity of Cl, $EA_{Cl^-} = 3.61$ eV, suggest an excess energy of reaction E_E of ~0.5 eV.

Figure 2 shows calculated position distributions for $K^+..Cl^-$ ion pairs produced through reaction (8) that travel within ±4° of the *xy* plane (the same angle as defined by the slit at the entrance to the analysis region). The figure includes results obtained when considering both total ion pair production and the production of ion pairs with binding energies $\lesssim$30 meV, as studied here. A laser pulse width of 1 μs is assumed in these calculations. The target gas pressures used in the gas cell, ~1 to 3×10^{-5} torr, result in collisional destruction rates ρk_a, where ρ is the target gas density and k_a the rate constant for low energy electron attachment, typically $\sim 10^{-7}$ cm^3 s^{-1}, of $\sim 10^5$ s^{-1}. This, coupled with the relatively short lifetime of the parent Rydberg state, ~4.4 μs, points to effective Rydberg lifetimes of ~3 μs. Thus, since the most probable Rydberg atom velocity is $\sim 5 \times 10^4$ cm s^{-1}, ion pair formation will typically occur within ~2 mm of the center of the gas cell. Therefore it is assumed in the calculations that all ion pairs are formed at the center of the gas cell. The calculations also presume that, as demonstrated in earlier studies,[11] the lifetimes of $K^+..Cl^-$ ion pairs are long, $\gg$100 μs.

The distributions predicted for total ion pair production assuming a δ-function translational energy release distribution with $\epsilon = 0.35$ eV are shown in Fig. 2. (Although this energy release is somewhat less than suggested by the available thermochemical data, it provides (as will be shown) an optimal fit to the experimental data.) The calculations also assume that the $C_2Cl_3F_3^{-*}$ intermediates are very short lived, $\tau = 0$, consistent with a large translational energy release. The results show that as the time delay t_D is increased the bound ion pairs move steadily away from their point of formation over a broad range of scattering angles focused in the forward ($\theta = 0$) direction with a range of speeds that for $\theta = 0$ is peaked near $\sim 1 \times 10^5$ cm s^{-1}. Calculations also showed that the arrival position distributions are insensitive to the assumed intermediate lifetime, τ, on time scales of less than a few tens of picoseconds, i.e., on time scales small compared to the orbital periods of $K^+..C_2Cl_3F_3^{-*}$ ion pairs, which is not unexpected, given that, on such timescales, any deflection of the trajectory of the K^+ core ion prior to dissociation is small compared to the angular width of the product ion pair distribution.

As the lifetime of the intermediate is increased, an increasing fraction of the excess energy E_E will be redistributed to internal motions in the intermediate prior to dissociation, resulting in a decrease in the mean energy that appears in translation. The effects of this are seen in Fig. 2

which includes results obtained using two different model translational energy release distributions: a flat rectangular distribution extending from 0 to 0.35 eV that allows for partial energy redistribution and the limiting case of a Boltzmann-like distribution with a mean translational energy release $\bar{\epsilon} = 0.05$ eV. Simple statistical arguments suggest that, in this limit, if the excess energy E_E is evenly distributed among the N internal modes of the intermediate, the mean translational energy release should be given by $\bar{\epsilon} = E_E/N$, which amounts to ~0.028 eV for $C_2Cl_3F_3$. However, earlier work has demonstrated that the mean translational energy release is frequently significantly larger than predicted by this simple expression,[21,22] an issue that has been addressed using re-formulated quasi-equilibrium theory.[23,24] As the mean translational energy release is reduced, the average velocity of the $K^+..Cl^-$ ion pairs decreases and their angular distributions become increasingly peaked in the forward direction. Again, the calculated angular distributions are relatively insensitive to the assumed intermediate lifetime on time scales of a few tens of picoseconds.

As is evident from Fig. 2, the calculated arrival position distributions for ion pair states with binding energies $\lesssim$30 meV differ significantly from those associated with total ion pair production. In particular, use of the Gaussian energy release distribution results in an angular distribution that is peaked at large scattering angles, $\theta \sim 45°$. Similar behavior is observed using the rectangular distribution, the angular distribution peaking at somewhat larger scattering angles. However, the arrival position distribution is again strongly forward peaked when assuming a Boltzmann-like distribution.

The general characteristics seen in Fig. 2 can be explained qualitatively by considering the kinetic energy of relative motion, E_{KREL}, of the K^+ and Cl^- ions immediately following the dissociation. For a δ-function translational energy release distribution, the velocity distribution of the Cl^- ions, which carry the bulk of the excess energy, is narrow and is centered (for $E_E = 0.35$ eV) near 1.4×10^5 cm s^{-1}, which is much larger than the most probable initial thermal velocity (in the laboratory frame) of the target molecules themselves, $\sim 1.6 \times 10^4$ cm s^{-1}, and of the Rydberg atoms which peaks at $\sim 5 \times 10^4$ cm s^{-1}. In consequence, the initial distribution of velocities of the Cl^- ions in the laboratory frame is relatively narrow. E_{KREL} is least, and hence the probability for creating a bound ion pair is greatest, when the K^+ and product Cl^- ions have similar velocities. Since, for short intermediate lifetimes, the K^+ ion trajectories are centered about the forward direction, this will result in an ion pair velocity distribution that is also peaked in the forward direction. The best velocity matching will be achieved for Rydberg atoms in the upper part of their velocity distribution leading to the formation of bound ion pairs with sizable translational velocities. As the angle, ϕ, between the initial direction of travel of the Cl^- fragment and the K^+ core ion increases so too, on average, does E_{KREL} resulting in a decrease in the fraction of ion pairs that remain bound and for those that do remain bound, a decrease in their binding energies. As ϕ increases, the $K^+..Cl^-$ ion pairs also acquire an increasing component of transverse momentum and are therefore scattered through increasing angles θ, which accounts for the broad calculated angular distribution of the ion pairs and why the angular distribution for the more weakly bound ion pairs is maximum at non-zero scattering angles. In the limit that $\phi \rightarrow 180°$, the K^+ and Cl^- ions are formed traveling in opposite directions which maximizes E_{KREL} and few ion pairs remain bound. Thus the angular distribution for *free* Cl^- ions is expected to peak in the backward direction as has been observed experimentally in earlier studies.[22,25] As the assumed mean translational energy release $\bar{\epsilon}$ is decreased, the initial velocities of the Cl^- fragments and their transverse components of momenta decrease. In consequence, velocity matching in the forward direction improves leading to a decrease in the average velocity of the product bound ion pairs and the angular distribution becomes increasingly forward peaked.

Fig. 3 shows measured arrival position distributions for $K^+..Cl^-$ ion pairs with binding energies $\lesssim$30 meV for a number of delay times t_D (measured from the end of the 10 μs-long laser pulse) together with the results of model calculations undertaken using a variety of different assumed translational energy release distributions. (The calculations assume constant Rydberg atom production/destruction rates during the laser pulse.) The white lines denote the area viewed by the PSD. To better emphasize the time dependence of the total ion signals associated with the different measured distributions, the distributions in each time-dependent series are normalized to the peak value seen within that series. (The same normalization procedure is applied in all later figures.) Figure 3 includes predicted arrival position distributions obtained using a narrow Gaussian translational energy distribution of 0.1 eV FWHM centered on the mean value $\bar{\epsilon} = 0.5$ eV. Use of this value leads to calculated ion-pair velocities that are significantly larger than observed, the product ion-pairs rapidly passing out of the analysis region. Use of a similar Gaussian distribution but with $\bar{\epsilon} = 0.35$ eV results in lower calculated ion-pair velocities and reasonable agreement with experiment suggesting that many capture events lead to direct dissociation, i.e., to the formation of very-short-lived intermediates although the excess energy of the reaction is a little less than that suggested by the thermochemical data. Careful inspection of the experimental data for the longer delay times, however, reveals that there is a low-velocity component present in the ion pair signal that is not predicted using a simple Gaussian distribution and which indicates that electron capture can lead to the formation of intermediates with lifetimes sufficient to allow at least partial redistribution of the excess energy within the intermediate prior to dissociation. To examine this further, Fig. 3 also contains the results of calculations that use a number of different trial translational energy release distributions which assume that some energy redistribution occurs within the intermediate prior to dissociation. The first, a triangular distribution that increases linearly with ϵ from zero at $\epsilon = 0$ to a cutoff at $\epsilon = 0.35$ eV, provides results that are also in reasonably good agreement with experiment although at the longer delay times, the ion pair arrival distribution is too strongly peaked at the larger scattering angles. Use of a triangular distribution that decreases linearly from a maximum at $\epsilon = 0$ to zero at $\epsilon = 0.35$ eV results in an arrival position distribution that, for the longest delay time, is fairly uniformly distributed across the PSD. Similar behavior is

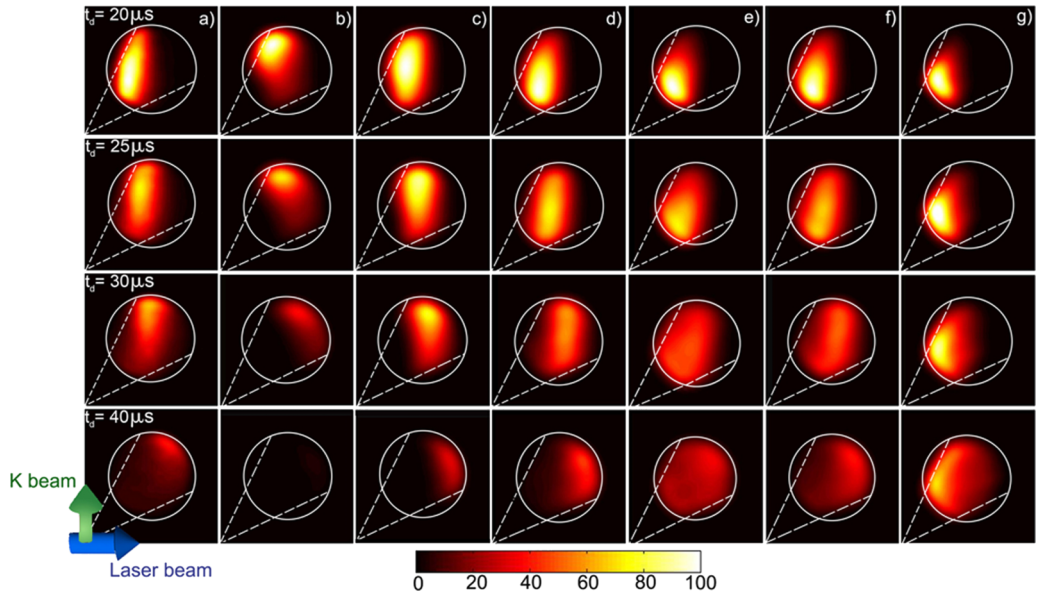

FIG. 3. (a) Measured arrival position distribution for $K^+..Cl^-$ ion pairs formed in K(12p)–$C_2Cl_3F_3$ collisions and the time delays t_D indicated. These, and all later, experimental data refer to the production of ion-pair states with binding energies $\lesssim$30 meV. The distributions in this, and later, time-dependent series are normalized to the peak value within the series. The figure also includes arrival positions derived assuming (b) a Gaussian distribution of 0.1 eV FWHM and $\bar{\epsilon} = 0.5$ eV, (c) the same distribution as in (b) but with $\bar{\epsilon} = 0.35$ eV, (d) a triangular distribution that increases linearly from 0 at $\epsilon = 0$ to a maximum at $\epsilon = 0.35$ eV, (e) a triangular distribution that decreases linearly from a maximum at $\epsilon = 0$ to 0 at $\epsilon = 0.35$ eV, (f) a rectangular distribution that extends from 0 to 0.35 eV, and (g) a Boltzmann-like distribution with $\bar{\epsilon} = 0.05$ eV.

seen using a rectangular distribution that extends from 0 to 0.2 eV. Were the lifetime of the intermediate sufficient to allow full statistical redistribution a Boltzmann-like distribution is expected. However, calculations for such a distribution with $\bar{\epsilon} = 0.05$ eV are included in Fig. 3 and have characteristics very different from those measured.

Good overall fits to the experimental data can be obtained by taking a linear combination of the distributions calculated for the Gaussian ($\bar{\epsilon} = 0.35$ eV) and (decreasing) triangular distribution. The quality of the fit that can be obtained in this manner is illustrated in Fig. 4 and also in Fig. 5 which shows the total ion signal recorded at the PSD as a function of time delay, together with the results of model calculations. Both figures include results calculated assuming different fractional contributions from each reaction channel. While the predicted results are not especially sensitive to the assumed fractional contributions, the data suggest that ~70%–90% of attachment events lead to direct dissociation, the remainder to the creation of intermediates with lifetimes sufficient to allow some internal redistribution of the excess energy prior to dissociation, i.e., with lifetimes of the order of a few vibrational periods, $\sim 10^{-13}$ to 10^{-12} s. These findings are consistent with those obtained in earlier studies of the velocity distribution of *free* Cl^- ions produced in Rydberg atom-$C_2Cl_3F_3$

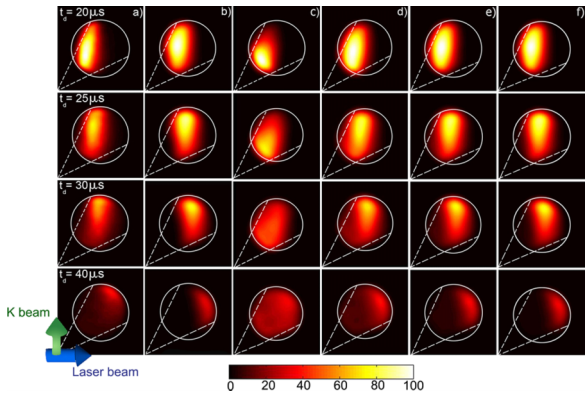

FIG. 4. (a) Measured arrival position distribution for $K^+..Cl^-$ ion pairs formed in K(12p)–$C_2Cl_3F_3$ collisions and the time delays t_D indicated. (b)-(d) Predictions of model calculations which assume that capture results from a combination of direct dissociation (DD) resulting in the translational energy release distribution seen in Fig. 3(c) and from partial redistribution (PR) of this energy to internal motions resulting in the distribution seen in Fig. 3(e). The percentage contributions from each channel are (b) 100% DD, (c) 100% PR, (d) 50% DD - 50% PR, (e) 70% DD - 30% PR, and (f) 85% DD - 15% PR.

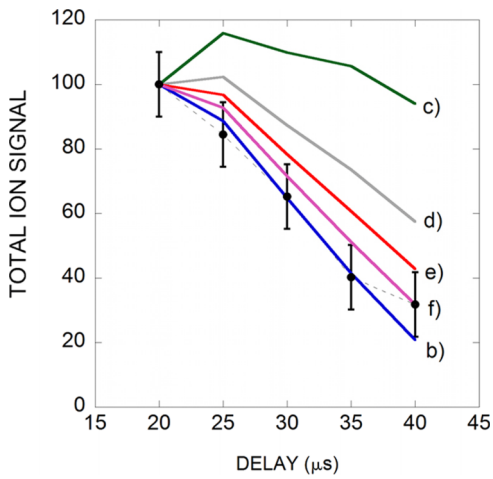

FIG. 5. •, total $K^+..Cl^-$ ion signal recorded at the PSD as a function of time delay. The lines show the results of model calculations that employ different relative contributions from the same two reaction channels as used in Fig. 4. The labels (b)–(f) correspond to the same relative contributions as in Fig. 4.

collisions undertaken at high n where post-attachment interactions are unimportant.[22] Theoretical analysis in this earlier work provided an explanation for the presence of two reaction channels. This analysis showed that the excess charge on the intermediate negative ion should reside primarily on the Cl_3 group, suggesting that electron capture at this end of the molecule is to be preferred. The production of the higher-velocity ion pairs can then be explained if capture at this end of the molecule leads to direct dissociation. Electron attachment to the F_3 group is also possible. However, the bond dissociation energy for the removal of an F atom from the parent molecule is large and there is insufficient energy available in Rydberg electron attachment to allow the creation of an F^- ion. Thus, following capture at the F_3 group, the electron must then transfer to the Cl_3 group allowing some time for energy redistribution within the intermediate.

B. $CBrCl_3$

Thermal electron attachment to $CBrCl_3$ can lead to the production of both Br^- and Cl^- ions, with Br^- production being dominant.[25,26] Thus electron transfer can result in the formation of both $K^+..Br^-$ and $K^+..Cl^-$ ion pairs through the reactions

$$K(12p) + CBrCl_3 \rightarrow K^+ + CBrCl_3^{-*} \rightarrow K^+..Br^- + CCl_3 \quad (9)$$

$$\rightarrow K^+..Cl^- + CBrCl_2. \quad (10)$$

These two reaction channels, however, cannot be separately identified using the present apparatus. Earlier Rydberg atom studies at high n point to a CCl_3–Br bond dissociation energy of ~2.7 eV, in good agreement with theoretical predictions.[27] Given the electron affinity of bromine, $EA_{Br^-} = 3.37$ eV, this points to an excess energy $E_E \sim 0.7$ eV for reaction (9). The $CBrCl_2$–Cl bond dissociation energy is less well known. Calculations suggest a value ~3.6 eV,[27] which is comparable to the electron affinity of chlorine, $EA_{Cl^-} = 3.61$ eV. The excess energy of reaction (10) is therefore expected to be small, $\lesssim$0.1 eV. Figure 6 shows measured arrival position distributions for ion pairs produced through a combination of reactions (9) and (10), together with the results of model calculations.

Consider initially the formation of $K^+..Br^-$ ion pairs which earlier measurements suggest should be the dominant reaction channel.[27] Use of a Gaussian distribution with a FWHM of 0.15 eV centered on $\bar{\epsilon} = 0.7$ eV yields predictions that are in poor agreement with experiment indicating that few capture events lead to Br^- production through direct dissociation. A Boltzmann-like distribution with $\bar{\epsilon} = 0.15$ eV, however, yields results that provide a good match to experiment pointing to the formation of an intermediate whose lifetime is sufficient to allow efficient redistribution of the excess energy prior to dissociation. The mean energy $\bar{\epsilon} = 0.15$ eV is again a little larger than suggested simply using E_E/N, i.e., ~0.08 eV, but is consistent with reformulated quasi-equilibrium theory.

Figure 6 also includes model calculations for the production of $K^+..Cl^-$ ion pairs. Earlier high-n studies showed that the data associated with Cl^- production could be well fit by assuming a Gaussian translational energy release distribution of 0.075 eV FWHM centered on 0.075 eV or a rectangular distribution with $\bar{\epsilon} = 0.075$ eV.[27] The earlier data, however, could not be well fit by assuming a Boltzmann-like distribution having any reasonable value of $\bar{\epsilon}$, which, given the small excess energy, should be $\lesssim$0.03 eV. As seen in Fig. 6, the present work is consistent with these earlier findings. The arrival position distributions agree well with predictions for the Gaussian

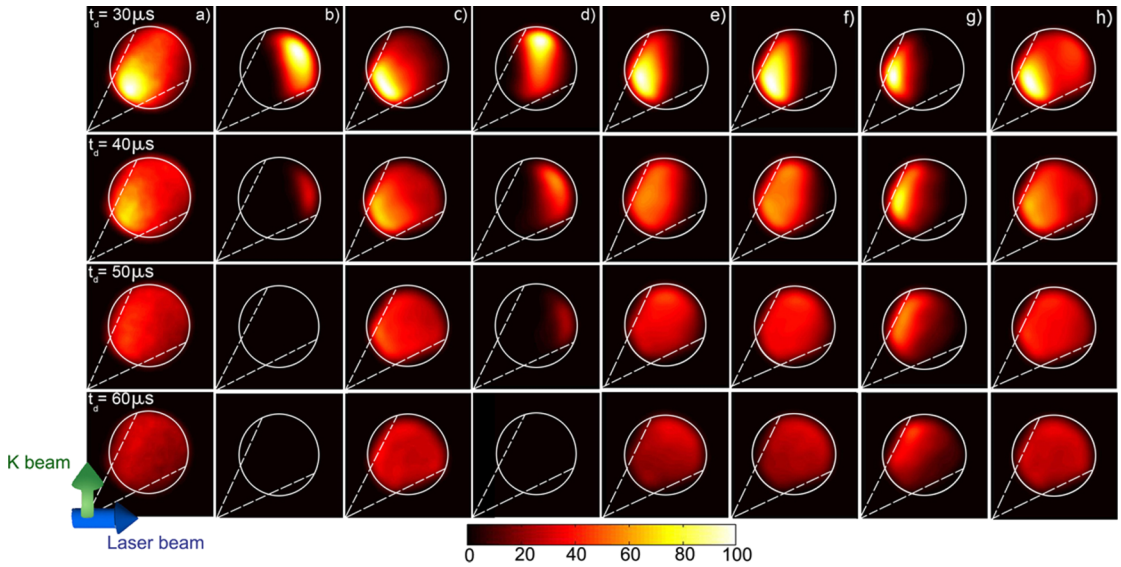

FIG. 6. (a) Measured ion-pair arrival position distributions for ion pairs produced in K(12p)–$CBrCl_3$ collisions via reactions (9) and (10). The figure includes separate model predictions for the formation of ((b) and (c)) $K^+..Br^-$ ion pairs and ((d)-(g)) $K^+..Cl^-$ ion pairs. These distributions assume (b) a Gaussian distribution of 0.015 eV FWHM centered on $\bar{\epsilon} = 0.7$ eV, (c) a Boltzmann-like distribution with $\bar{\epsilon} = 0.15$ eV, (d) a Gaussian distribution of 0.075 eV FWHM centered on $\epsilon = 0.3$ eV, (e) a Gaussian distribution of 0.075 eV FWHM centered on 0.075 eV, (f) a rectangular distribution with $\bar{\epsilon} = 0.075$ eV, and (g) a Boltzmann-like distribution with $\bar{\epsilon} = 0.03$ eV. (h) Predictions of model calculations which assume that 70% (30%) of attachment events lead to $K^+..Br^-$ ($K^+..Cl^-$) formation via a long-lived (short-lived) intermediate state (see text).

(and rectangular) distributions but not the Boltzmann-like distribution. Interestingly, earlier studies[25] have also pointed to the existence of a channel that results in a Gaussian energy release distribution centered on $\bar{\epsilon} = 0.3$ eV with a FWHM of 0.15 eV, but as is evident from Fig. 6, the present results reveal little evidence for the presence of such a channel. The present data thus suggest that the lifetime of the CCl_3Br^{-*} intermediate associated with Cl^- production is short and insufficient to allow full statistical redistribution of the excess energy prior to dissociation.

Good overall fits to the data can be obtained by assuming that ~70% of collisions lead to production of $K^+..Br^-$ ion pairs through formation of a long-lived intermediate, and ~30% to creation of $K^+..Cl^-$ ion pairs via a short-lived intermediate. The present results therefore point to a reaction model in which direct capture at a Cl site leads to immediate, or at least very rapid, dissociation. (Earlier theory suggests that a large fraction of the excess charge on the intermediate is located on the Cl atoms and is antibonding with respect to the C–Cl bond.[27]) However, the excess energy E_E associated with Cl^- production is small, and free-electron studies have suggested the presence of a small potential barrier of ~50 meV to Cl^- formation.[28] This will reduce the probability for direct dissociation allowing transient binding and energy redistribution within the intermediate whereupon subsequent dissociation will favor the formation of Br^- ions due to their weaker binding.

C. BrCN

Electron transfer to BrCN results in ion pair formation via the reaction

$$K(12p) + BrCN \rightarrow K^+ + BrCN^{-*} \rightarrow K^+..CN^- + Br. \quad (11)$$

Thermochemical and photodissociation measurements point to a Br–CN bond dissociation energy of ~3.70 eV.[29–31] Since the electron affinity of the CN radical is $EA_{CN^-} = 3.86$ eV, this suggests an excess energy of reaction $E_E \sim 0.2$ eV.

Figure 7 shows the measured arrival position distributions for the $K^+..CN^-$ ion pairs together with the results of model calculations. Earlier measurements of ion-pair lifetimes, however, have shown that weakly bound $Br^+..CN^-$ ion pairs have finite lifetimes. Whereas ion pairs with binding energies, E_B, >30 meV have long lifetimes $\gtrsim$100 μs, states with $E_B \sim 20$ meV decay with mean lifetimes of ~25 μs, and these being reduced to ~7 μs for values of $E_B \sim 9$ meV.[11] These binding-energy-dependent ion-pair lifetimes are taken into account in the model calculations. The results of calculations undertaken assuming a Gaussian energy release distribution with a FWHM of 0.05 eV centered on $\bar{\epsilon} = 0.2$ eV are shown in Fig. 7 and are in poor agreement with experiment, the predicted ion pair velocities are larger than measured, and their angular distribution is peaked at larger scattering angles. These differences indicate that electron capture by BrCN does not lead to direct dissociation and point to an excess energy E_E that is significantly less than 0.2 eV. Earlier measurements of CN^- radial arrival position distributions following K(55p)–BrCN collisions suggested an energy release distribution in the form of a Gaussian distribution with a FWHM of 0.05 eV

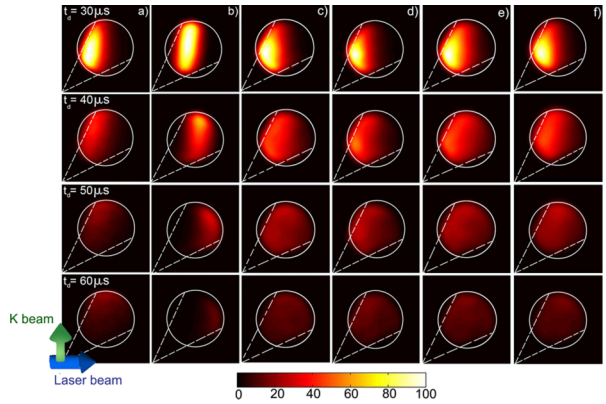

FIG. 7. (a) Measured ion-pair arrival position distributions for $K^+..CN^-$ ion pairs formed in K(12p)–BrCN collisions. The figure includes model predictions obtained using the measured $K^+..CN^-$ ion pair lifetimes assuming (b) a Gaussian distribution of 0.05 eV FWHM centered on $\bar{\epsilon} = 0.2$ eV, (c) a Gaussian distribution of 0.05 eV FWHM centered on $\bar{\epsilon} = 0.1$ eV, (d) and (e) Boltzmann-like distributions with $\bar{\epsilon} = 0.05$ and 0.1 eV, respectively, and (f) a distribution that assumes an excess energy $E_E = 0.14$ eV and a CN^- rotational temperature of 600 K (see text).

centered on 0.1 eV.[25] However, as seen in Fig. 7, whereas use of such a distribution yields reasonable agreement with experiment, differences remain. Similar differences remain when comparing results obtained assuming Boltzmann-like translational energy release distributions with mean energies of $\bar{\epsilon} = 0.05$ eV and 0.1 eV and a mean $BrCN^{-*}$ intermediate lifetime of 20 ps. Differences with the predictions for a Boltzmann-like distribution are not unexpected because, if the excess energy E_E does not appear in translation, it must appear in rovibrational excitation of the CN^- fragment. However, E_E is less than the calculated vibrational spacing for CN^- ions, ~0.25 eV.[32] Given that the vibrational spacing for the C–N stretch mode in BrCN is sizable, ~0.27 eV, this mode is not significantly excited in a room-temperature target. Thus the CN^- ions must be formed in their ground vibrational state and the excess energy must appear in rotational excitation of the CN^- fragment. In this event, a Boltzmann-like distribution would require the preferential population of high rotational states. The rotational constant for CN^- is small, B ~ 0.23 meV,[33] and the conversion of 0.1 to 0.2 eV into rotational motion would require a mechanism to preferentially populate states with $J \sim 20$–30 and such mechanisms are difficult to envision. Somewhat better fits to the data can be obtained using translational energy release distributions that model the production of CN^- ions having suprathermal rotational energy distributions. This is illustrated in Fig. 7 which includes the results of calculations that assume an excess energy of reaction of 0.14 eV and a CN^- rotational temperature of 600 K. While the predicted distributions are not especially sensitive to the assumed rotational temperature over the range 450–900 K, the results do indicate that electron attachment to BrCN leads to the creation of CN^- ions in a broad range of rotationally excited states. This finding is consistent with the results of threshold ion pair production spectroscopy studies of HCN which also showed the CN^- fragments to be rotationally hot.[34] In addition, rotational excitation can account for the short lifetimes of weakly bound

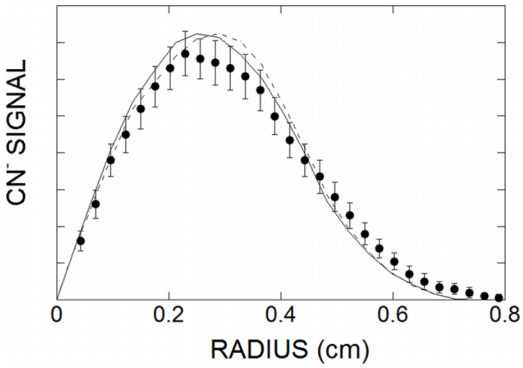

FIG. 8. Radial arrival position distribution for CN^- ions produced in K(55p)–BrCN collisions (taken from Ref. 25). •, experimental data. The lines show distributions calculated assuming the same distributions as in Fig. 7(c) (- - - -) and Fig. 7(f) (——).

$K^+..CN^-$ ion pairs since conversion of rotational energy in the CN^- ion into internal motions of the ion pair can lead to dissociation. The energy release distribution suggested here is rather different from the Gaussian distribution inferred from earlier measurements of radial velocity distributions at high n.[25] However, as illustrated in Fig. 8, the present distribution provides a somewhat better fit to the earlier results.

D. $Fe(CO)_5$

Rydberg atom collisions with $Fe(CO)_5$ lead to the formation of ion pair states via the reaction

$$\begin{aligned} K(12p) + Fe(CO)_5 &\rightarrow K^+ + Fe(CO)_5^{-*} \\ &\rightarrow K^+..Fe(CO)_4^- + CO. \end{aligned} \quad (12)$$

Values of 1.8 ± 0.5 eV and 2.4 ± 0.3 have been reported for the $Fe(CO)_4$–CO bond dissociation energy and the electron affinity of $Fe(CO)_4$, respectively.[35,36] This suggests an excess energy $E_E \sim 0.6$ eV, although the large uncertainties admit a broad range of possible values. Better defining this value through studies of Rydberg electron transfer, however, is challenging because the mass of the $Fe(CO)_4^-$ fragment is much greater than that of the neutral CO fragment and upon dissociation a large fraction of the translational energy released is acquired by the CO fragment. In consequence, the final velocity of the anion is little changed from that of the parent molecule resulting in calculated ion-pair arrival distributions that are relatively insensitive to the particular choice of translational energy release distribution.

Figure 9 shows the measured ion pair arrival position distributions together with those predicted assuming different translational energy release distributions. A reasonable fit to the experimental data can be achieved using a Boltzmann-like distribution, the best agreement being obtained for values of $\bar{\epsilon} \sim 0.2$ eV. A Boltzmann-like distribution, however, requires energy redistribution within the intermediate prior to dissociation and the creation of negative ions with considerable internal energy. As demonstrated in earlier studies of $K^+..SF_6^-$ ion pairs, transfer of internal energy from a (molecular) negative ion into translational motions

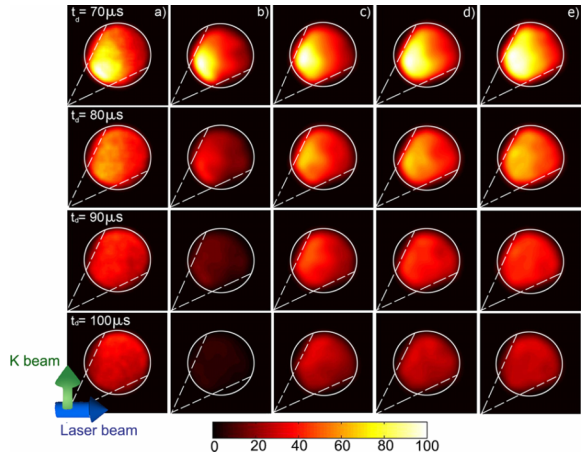

FIG. 9. (a) Measured ion pair arrival position distributions for $K^+..Fe(CO)_4^-$ ion pairs formed in K(12p)–$Fe(CO)_5$ collisions. The figure includes model predictions obtained assuming Boltzmann-like distributions with $\bar{\epsilon} = 0.2$ eV and (b) ion-pair lifetimes equal to those of $K^+..SF_6^-$ ion pairs, (c) a fixed lifetime $\tau = 50$ μs (see text), (d) a rectangular distribution with $\bar{\epsilon} = 0.2$ eV and $\tau = 50$ μs, and (e) a Gaussian distribution of 0.05 eV FWHM centered on $\epsilon = 0.2$ eV and $\tau = 50$ μs.

of the ion pair can lead to dissociation and reduced ion-pair lifetimes.[11] These lifetimes can be further reduced through near-resonant charge transfer in close encounters between the ion pair. However, as is apparent from Fig. 9, use of the lifetimes reported earlier for $K^+..SF_6^-$ ion pairs, which decreased from ~18 μs for a binding energy of ~7 meV to ~9 μs for a binding energy of ~30 meV, yields results in poor agreement with experiment, the predicted ion pair signal decreasing much more rapidly with increasing flight time than is observed. The best fits to the data are obtained assuming somewhat longer ion pair lifetimes of ~50 μs. However, if complete statistical redistribution of the excess energy were to occur prior to dissociation, this would point to an excess energy $E_E \sim N\bar{\epsilon} \sim 5$ eV. Even though such simple statistical estimates frequently underestimate the energy release, the use of a Boltzmann-like distribution appears inappropriate as it requires a value of E_E well outside the anticipated range. Partial energy redistribution within the intermediate is still possible and is modeled using a rectangular distribution. The best fits to the experimental data are obtained using a distribution that extends from 0 to ~0.4 eV, i.e., that has a mean energy $\bar{\epsilon} = 0.2$ eV, and an ion pair lifetime of ~50 μs. The present measurements can also be well fit using a Gaussian distribution. However, since the room-temperature target molecules themselves contain significant internal energy, ~0.25 eV, even following direct dissociation, the negative ion would still possess sufficient internal energy to induce dissociation and reduce the ion-pair lifetimes. Good fits are obtained by assuming a Gaussian distribution centered near $\bar{\epsilon} \sim 0.2$ eV with a FWHM of ~0.05 eV and an ion-pair lifetime of again ~50 μs. Use of larger mean energies leads to rapidly worsening agreement with experiment. Taken together the data suggest that electron attachment to $Fe(CO)_5$ leads to direct, or very rapid (on time scales of a few vibrational periods), dissociation. The data also point to a small excess energy of reaction, $E_E \lesssim 0.4$ eV.

IV. CONCLUSIONS AND FUTURE DIRECTIONS

The present work demonstrates that measurements of the velocity distribution of heavy-Rydberg ion-pair states formed through dissociative electron transfer in low-n Rydberg atom collisions provide a window into the dynamics of electron transfer and highlight the variety of different behaviors that accompany dissociative electron attachment. For example, in the case of 1,1,1-$C_2Cl_3F_3$, the data show that electrons can be captured directly into antibonding orbitals leading to direct dissociation with all the excess energy of reaction appearing in translational energy of the products. Capture by this molecule, however, is also seen to lead to the production of excited intermediates with lifetimes of a few vibrational periods sufficient to allow partial energy redistribution within the intermediate prior to dissociation. Even longer intermediate lifetimes are observed for $CBrCl_3$ where the lifetime of the intermediates involved in the formation of $K^+..Br^-$ ion pairs is sufficient to permit near-statistical redistribution of the excess energy within the intermediate prior to dissociation. The data for BrCN also point to the formation of relatively long-lived intermediates which upon dissociation produce rotationally hot CN^- ions. The results for $Fe(CO)_5$ are consistent with the formation of short-lived intermediates.

In the future, the level of detailed information that might be obtained from Rydberg atom measurements can be substantially improved by better defining the initial collision conditions. One way to achieve this is to use velocity-selected Rydberg atoms. Such atoms can be created by arranging that the laser beam is incident at a small angle (~2°) off-normal to the atom beam and tuning the laser to the desired position in the resulting Doppler profile. While this will lead to a sizable reduction in the Rydberg atom production rate, recent work suggests that this can be more than compensated for by use of strontium which offers very much higher Rydberg production rates than can be easily achieved in potassium.[37] Better definition of the initial conditions can also be achieved by replacing the gas cell by a target cross beam. Further improvements might be obtained by modifying the analysis region to permit application of larger dissociation fields which would allow studies of ion pair states with higher binding energies and, when coupled with the higher excitation rates afforded by strontium, would allow measurements involving ion-pair states with limited ranges of binding energy.

ACKNOWLEDGMENTS

Research supported by the Robert A. Welch Foundation under Grant No. C-0734.

[1]F. B. Dunning, in *Photonic, Electronic and Atomic Collisions*, edited by P. D. Fainstein *et al.* (World Scientific, 2006), pp. 64–75.
[2]F. B. Dunning, J. Phys. B: At., Mol. Opt. Phys. **28**, 1645 (1995).
[3]E. Reinhold and W. Ubachs, Phys. Rev. Lett. **88**, 013001 (2001).
[4]R. C. Shiell, E. Reinhold, F. Magnus, and W. Ubachs, Phys. Rev. Lett. **95**, 213002 (2005).
[5]E. Reinhold and W. Ubachs, Mol. Phys. **103**, 1329 (2005).
[6]M. O. Vieitez, T. I. Ivanov, E. Reinhold, C. A. de Lange, and W. Ubachs, Phys. Rev. Lett. **101**, 163001 (2008).
[7]S. Mollet and F. Merkt, Phys. Rev. A **82**, 032510 (2010).
[8]M. Cannon, Y. Liu, and F. B. Dunning, Chem. Phys. Lett. **458**, 35 (2008).
[9]M. Cannon and F. B. Dunning, J. Chem. Phys. **130**, 044304 (2009).
[10]M. Cannon, C. H. Wang, and F. B. Dunning, Chem. Phys. Lett. **479**, 30 (2009).
[11]M. Cannon, C. H. Wang, F. B. Dunning, and C. O. Reinhold, J. Chem. Phys. **133**, 064301 (2010).
[12]C. H. Wang, M. Kelley, S. Buathong, and F. B. Dunning, J. Chem. Phys. **140**, 234306 (2014).
[13]S. Buathong, M. Kelley, C. H. Wang, and F. B. Dunning, Chem. Phys. Lett. **618**, 153 (2015).
[14]M. Kelley, S. Buathong, and F. B. Dunning, J. Phys.: Conf. Ser. **635**, 012024 (2015).
[15]C. O. Reinhold, S. Yoshida, and F. B. Dunning, J. Chem. Phys. **134**, 174305 (2011).
[16]X. Ling, M. A. Durham, A. Kalamarides, R. W. Marawar, B. G. Lindsay, K. A. Smith, and F. B. Dunning, J. Chem. Phys. **93**, 8669 (1990).
[17]C. E. Klots, J. Chem. Phys. **41**, 117 (1964).
[18]P. J. Robinson and K. A. Holbrook, *Unimolecular Reactions* (Wiley-Interscience, London, New York, 1972).
[19]D. Manura and D. Dahl, *SIMION (R) 8.0 User Manual* (Scientific Instrument Services, Inc., Ringoes, NJ, 2008).
[20]Y.-R. Luo, *Handbook of Bond Dissociation Energies in Organic Compounds* (CRC, Boca Raton, FL, 2002).
[21]E. L. Spotz, W. A. Seitz, and J. L. Franklin, J. Chem. Phys. **51**, 5142 (1969).
[22]C. D. Finch, R. Parthasarathy, H. C. Akpati, P. Nordlander, and F. B. Dunning, J. Chem. Phys. **106**, 9594 (1997).
[23]C. E. Klots, J. Chem. Phys. **75**, 1526 (1971).
[24]C. E. Klots, Z. Naturforsch. A **27**, 553 (1972).
[25]R. Parthasarathy, L. Suess, S. B. Hill, and F. B. Dunning, J. Chem. Phys. **114**, 7962 (2001).
[26]E. P. Grimsrud and S. H. Kim, Anal. Chem. **51**, 537 (1979).
[27]R. Parthasarathy, C. D. Finch, J. Wolfgang, P. Nordlander, and F. B. Dunning, J. Chem. Phys. **109**, 8829 (1998).
[28]P. Spanel, D. Smith, S. Matejcik, A. Kiendler, and T. Märk, Int. J. Mass Spectrom. Ion Processes **167/168**, 1 (1997).
[29]F. Brüning, I. Hahndorf, A. Stamatovic, and E. Illenberger, J. Chem. Phys. **100**, 19740 (1996).
[30]J. Berkowitz, J. Chem. Phys. **36**, 2533 (1962).
[31]D. D. Davis and H. Okabe, J. Chem. Phys. **49**, 5526 (1968).
[32]C. W. Bauschlicher, Int. J. Quantum Chem. **61**, 859 (1997).
[33]C. A. Gottlieb, S. Brünken, M. C. McCarthy, and P. Thaddeus, J. Chem. Phys. **126**, 191101 (2007).
[34]Q. J. Hu, Q. Zhang, and J. W. Hepburn, J. Chem. Phys. **124**, 074310 (2006).
[35]K. E. Lewis, D. M. Golden, and G. P. Smith, J. Am. Chem. Soc. **106**, 3905 (1984).
[36]P. C. Engelking and W. C. Lineberger, J. Am. Chem. Soc. **101**, 5569 (1979).
[37]S. Ye, X. Zhang, F. B. Dunning, S. Yoshida, M. Hiller, and J. Burgdörfer, Phys. Rev. A **90**, 013401 (2014).